Order parameter saturation in $LaAlO_3$

2002 J. Phys.: Condens. Matter 14 10131

(http://iopscience.iop.org/0953-8984/14/43/311)

INSTITUTE OF PHYSICS PUBLISHING JOURNAL OF PHYSICS: CONDENSED MATTER

J. Phys.: Condens. Matter **14** (2002) 10131–10144 PII: S0953-8984(02)36806-1

Order parameter saturation in $LaAlO_3$

S A Hayward, S A T Redfern and E K H Salje

Department of Earth Sciences, University of Cambridge, Downing Street, Cambridge CB2 3EQ, UK

E-mail: sah21@esc.cam.ac.uk

Received 9 May 2002, in final form 1 July 2002
Published 18 October 2002
Online at stacks.iop.org/JPhysCM/14/10131

Abstract

High-resolution x-ray rocking diffraction has been used to measure the spontaneous strain associated with the cubic–rhombohedral phase transition in $LaAlO_3$ in the range 10 K $\leqslant T \leqslant$ 750 K. The data are consistent with a second-order Landau-like model at high temperatures, with $T_C = 834(2)$ K. At lower temperatures, the strain data display order parameter saturation, related to the quantum saturation of the phonon modes. Comparison of the saturation temperature for the spontaneous strain ($\theta_S = 95$ K) with the saturation temperatures for independent measurements of the rotation ($\theta_S = 260$ K) and distortion ($\theta_S = 150$ K) of the AlO_6 octahedra indicates that the phase transition consists of two coupled processes, and that the coupling does not have the same effect in the classical and quantum saturation limits.

1. Introduction

Lanthanum aluminate, $LaAlO_3$, is rhombohedral at room temperature, and undergoes a phase transition to the cubic perovskite aristotype structure at $T_C \approx 850$ K. The spontaneous strain is small (0.6% at room temperature) (Geller and Bala 1956), and linear with temperature between room temperature and T_C (Chrosch and Salje 1999).

In recent years there have been a number of studies of the behaviour of $LaAlO_3$ as a function of temperature. A range of techniques has been used, including neutron powder diffraction (Chakoumakos *et al* 1998, Lehnert *et al* 2000, Howard *et al* 2000), x-ray diffuse scattering (Chrosch and Salje 1999) and differential scanning calorimetry (Beuble *et al* 1998). There have been additional studies of $LaAlO_3$ at room temperature, including infra-red and Raman spectroscopy (Abrashev *et al* 1999) and scanning force microscopy (Beuble *et al* 1998).

These studies have been motivated by several factors. One is to study $LaAlO_3$ in the context of other rhombohedral perovskites, such as $LaGaO_3$, $PrAlO_3$ and $NdAlO_3$ (Howard *et al* 2000). These other perovskites are all rhombohedral at moderate temperatures, and tend towards the cubic structure on heating. However, $LaAlO_3$ is unusual in undergoing the rhombohedral–cubic phase transition at a relatively low temperature.

Another reason for recent interest in $LaAlO_3$ is its potential use as a substrate for superconducting thin films. Although the structural match between $LaAlO_3$ and YBCO is not as good as for a number of other substrate materials, it has the additional benefit of a low dielectric constant. This property is useful in microwave applications.

The question of whether $LaAlO_3$ has a significant temperature range over which critical fluctuations modify the order parameter Q is, to an extent, still an open one. The Q^2 versus temperature data of Chrosch and Salje (1999) do not, within experimental resolution, show any deviations from linearity close to T_C. On the other hand some (but not all) of the data of Lehnert *et al* (2000) show pronounced curvature, but cover a much more limited number of points in a rather narrow temperature range. Such experiments are admittedly difficult, since the deviation from the ideal cubic perovskite structure is so small.

A further complication is that two crystal-structure-scale processes are associated with the breaking of the cubic symmetry. The AlO_6 octahedra rotate around the triad axis, and also change their shape, becoming shorter along the triad axis and elongated perpendicular to this axis. These lead to two separate spontaneous strains each arising below the phase transition.

In this study, we report the results of new high-resolution x-ray rocking experiments on $LaAlO_3$, which have been used to determine the spontaneous strain in the temperature range $10\ \mathrm{K} < T < 850\ \mathrm{K}$. These results are interpreted in terms of Landau theory, including the quantum mechanical modification at low temperatures. A consistent description of the phase transition requires the two transition processes to have different saturation temperatures.

2. Theory

2.1. Origin of thermodynamic saturation

Although the high-temperature behaviour of $LaAlO_3$ follows the predictions of a simple 2:4 Landau potential very well, it is known that this model cannot simply be extrapolated to lower temperatures. The underlying difficulty lies in the third law of thermodynamics, which implies that absolute zero temperature cannot be attained. A direct consequence of this is that $\partial Q/\partial T \rightarrow 0$ as $T \rightarrow 0$. The saturation behaviour is driven by thermodynamic effects, and not because the order parameter has reached some maximum value, which can never be exceeded. The contrast here is with cation ordering transitions, or a hypothetical displacive transition with strong stereochemical constraints.

It has been shown (Salje *et al* 1991, Dove *et al* 1992) that the key feature of the classical Landau potential, that the excess entropy ΔS is proportional to Q^2, follows from more general physical models provided that certain approximations are made. These approximations are valid for large values of T, and are equivalent to the approximations made when deriving classical physics from more general quantum mechanical models. Thus the quantum Landau potential (Salje *et al* 1991),

$$\Delta G = \frac{A\theta_S}{2}\left(\coth\left(\frac{\theta_S}{T}\right) - \coth\left(\frac{\theta_S}{T_C}\right)\right)Q^2 + \frac{B}{4}Q^4 + \cdots, \tag{1}$$

is equivalent to the classical Landau potential

$$\Delta G = \frac{A}{2}(T - T_C)Q^2 + \frac{B}{4}Q^4 + \cdots, \tag{2}$$

when T is at least moderately large relative to θ_S.

In equation (1), the transition is characterized by two temperatures, θ_S and T_C. Traditionally, studies of phase transitions have focused on T_C. However, determinations of θ_S may also yield useful insights into the behaviour of phase transitions. An important point is

that, unlike T_C, it seems that θ_S is not greatly altered by chemical doping, or the application of external fields (Hayward and Salje 1998). This point leads to the possibility that θ_S may actually be a more useful parameter for characterizing phase transitions than T_C. However, before θ_S values can be used in this way, an understanding of the principles which determine what θ_S is for a given phase transition is needed.

Pérez-Mato and Salje (2001), following the approach of Salje *et al* (1991), developed the formal quantum mechanical calculation of θ_S by calculating the effect of coupling a branch of Einstein oscillators (in other words, the hard modes) to a set of interacting quantum oscillators (i.e. the soft mode of the transition). Such a picture is applicable to the situation where the soft mode is an optic mode—which is the case in $LaAlO_3$.

The results of these calculations are conveniently shown by considering the behaviour of a limiting second-order phase transition subject to quantum effects. Thus, whereas in the classical second-order Landau potential the temperature dependence of the order parameter is

$$Q^2 = 1 - (T/T_C), \tag{3}$$

the equivalent expression when quantum saturation is included in the calculation is

$$Q^2 = 1 - \frac{1}{T_C}\left(\theta_S \coth\left(\frac{\theta_S}{T}\right)\right). \tag{4}$$

If the soft mode and the various hard modes are considered independently, equation (4) becomes

$$Q^2 = 1 - \frac{\theta_{S0}}{T_C}\left(\coth\left(\frac{\theta_{S0}}{T}\right) + \sum_j \frac{W_j \theta_{S0}}{12 E_0 \theta_{Sj}} \coth\left(\frac{\theta_{Sj}}{T}\right)\right), \tag{5}$$

where θ_{S0} is the saturation temperature for the soft mode, θ_{Sj} is the saturation temperature for the hard mode j, and (W_j/E_0) is the coupling energy between the soft mode and the hard mode j, relative to the energy of the local intersite interactions. Typically, (W_j/E_0) is expected to be of the order of unity. In this case, the contribution to the order parameter saturation of the summation over the hard modes will be very small compared with the soft mode, even though there will generally be many more hard than soft modes.

The saturation temperature for the order parameter is thus expected to be similar to the saturation temperature of the bare soft mode, which depends on its bare frequency. Experimental determination of this quantity is not straightforward, since any measurement of the soft mode frequency will be affected by the proximity to the phase transition. In the case of quartz, computer modelling has been used to attempt to determine θ_{S0} from the underlying atomistic potentials (Dove *et al* 1999, Salje 2000). These calculations yield sensible, but not quantitatively exact values for θ_{S0}; in the case of quartz, calculations based on lattice dynamics give the bare soft mode frequency as 71 cm^{-1}, corresponding to $\theta_S = 102$ K. The primary value of θ_S found experimentally in quartz (Salje 2000, Romero *et al* in preparation) is 180 K.

This approach contrasts strongly with the description of the saturation of other thermodynamic variables, such as specific heat and thermal expansion of solids. The standard result (see, for example, Born and Huang (1954)) is that all phonon modes contribute with equal weighting to the saturation of the specific heat and thermal expansion. Making appropriate assumptions about the shape of the phonon density of states function (such as the Einstein or Debye models) allows the entire phonon spectrum to be characterized by a single frequency, which is in some sense an average over all the phonon modes. Such an average is inevitably dominated by the hard modes, and so does not change significantly with temperature. We then find, for example, that the bare thermal expansion of a solid, expressed as the temperature

dependence of the lattice parameter a, is given, assuming Einstein-like specific heat and a constant Grüneisen parameter, by

$$a = a_0 + a_1 \int_0^T \left(\frac{\theta_E}{T}\right)^2 \frac{\exp(\theta_E/T)}{[\exp(\theta_E/T) - 1]^2}\,\mathrm{d}T. \tag{6}$$

Numerical integration of equation (6) shows that it is well approximated by

$$a = a_0 + a_1\theta_S \coth(\theta_S/T), \tag{7}$$

with $\theta_S = \theta_E/2$. The attractive feature of the form of $a(T)$ in equation (7) is its analogy to the form of $Q^2(T)$ in equation (4). As a result, we can meaningfully compare the values of θ_S obtained for the bare thermal expansion (which samples the entire phonon heat bath uniformly) and θ_S for the phase transition (which, in general, does not).

2.2. *Crystallography of $LaAlO_3$ and spontaneous strain expressions*

The space group of the low-temperature form of $LaAlO_3$ is $R\bar{3}c$, for which two sets of crystallographic axes are in common use. For many purposes, the most convenient system of axes is trigonal ($a = b \approx c/\sqrt{6}; \alpha = \beta = 90°, \gamma = 120°$). For the cubic–rhombohedral phase transition in $LaAlO_3$ these axes are particularly useful, since the axis around which the AlO_6 octahedra rotate, and along which they distort, is [001]. Following the argument of Megaw and Darlington (1975), the changes in the lattice parameters in the trigonal system, a_T and c_T, are simple functions of the two phase transition processes. Using the notation of Howard and Kennedy (1999) and Howard *et al* (2000), the octahedral distortion is given by the parameter η, where $\eta > 1$ implies that the octahedra are elongated along the trigonal z axis. The octahedra rotate around this axis, through an angle ϕ. Using the trigonal reference axes, the ratio a_T/c_T is then given by

$$\frac{a_T}{c_T} = \frac{\cos\varphi}{\eta\sqrt{6}}. \tag{8}$$

The alternative crystallographic description of the $R\bar{3}c$ structure is to use a pseudocubic unit cell ($a = b = c; \alpha = \beta = \gamma \approx 90°$). The advantage of describing the structure in this way is that the spontaneous strains associated with the cubic–trigonal phase transition have a more physically intuitive form. The key point, discussed by Carpenter *et al* (1998), is the need to adapt the spontaneous strains to properly reflect the way that the phase transition breaks the cubic symmetry. Whilst this can be done using spontaneous strains referred to the trigonal axes, it is more elegant to quantify the structural changes using the pseudocubic description of the $LaAlO_3$ structure.

The two free lattice parameters in the pseudocubic cell are a_P and α_P, and the spontaneous strain components are e_1 and e_4:

$$e_1 = \frac{a_P}{a_{P0}} - 1, \tag{9}$$

where a_{P0} is the value of a extrapolated from the high-temperature phase, neglecting the effects of the phase transition, and

$$e_4 \approx \frac{a_P}{a_{P0}} \cos\alpha_P. \tag{10}$$

The advantage of expressing the spontaneous strains in this form is that e_1 and e_4 are pure non-symmetry breaking and symmetry-breaking strains respectively.

Following from this, the twin angle measured in an x-ray rocking experiment measures e_4 only. The geometry of the rocking experiment is shown in figure 1. In the rocking experiment,

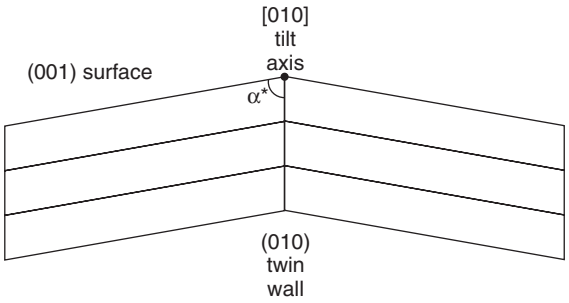

Figure 1. Sketch of real-space crystallography of (010) twins in rhombohedral $LaAlO_3$. The pseudocubic axes are used; $a = b = c$, $(\alpha = \beta = \gamma) \neq 90°$.

we tilt the crystal around [100] to measure the angle between the diffraction positions for the (001) planes in the two domains. This angle, $\Delta\omega = 2|90° - \alpha^*|$. Thus $\sin(\Delta\omega/2) = |\cos\alpha^*|$. For small values of the strain, $\cos\alpha \approx \cos\alpha^*$ and $\sin(\Delta\omega/2) \approx \Delta\omega/2$. We thus get the result $\Delta\omega = 2|e_4|$.

To see how the twin angle depends on the rotation and distortion of the octahedra, it is convenient to start with equation (8) above, and then convert the lattice parameters of the trigonal cell to the pseudocubic cell. The $\{100\}$ planes (on the pseudocubic axes) are equivalent to $\{102\}$ on the trigonal axes. Since α_P^* is the angle between the (100) and (010) planes, we have

$$\cos\alpha_P^* = \left(\frac{3a_T^2}{c_T^2} - \frac{1}{2}\right) \Big/ \left(\frac{3a_T^2}{c_T^2} + 1\right) \tag{11}$$

and so

$$\sin\frac{\Delta\omega}{2} = \cos\alpha_P^* = \frac{\frac{\cos^2\phi}{2\eta^2} - \frac{1}{2}}{1 + \frac{\cos^2\phi}{2\eta^2}} \tag{12}$$

which, for small rotations and distortions simplifies to

$$\Delta\omega = 2|e_4| = \tfrac{2}{3}|2(\eta - 1) + \phi^2|. \tag{13}$$

3. Experimental details

3.1. Sample description

Single crystals of $LaAlO_3$ were taken from a routine batch prepared by Crystal GmbH, Berlin, Germany. Referenced to the pseudocubic axes, the sample was a ground and polished (001) slice, predominantly containing $\{100\}$ twins. A piece approximately 2 mm × 2 mm × 0.5 mm was cut from this slice for mounting on each diffractometer. Characteristic optical micrographs of the as-received samples are shown in figure 2.

It has previously been noted that $LaAlO_3$ samples which have been heated above the rhombohedral–cubic transition temperature and subsequently recooled have a dramatically different microstructure (Beuble *et al* 1998). Figure 3 shows examples of the twin microstructure after heating. Unlike the predominantly lamellar twins in figure 2, the crossed twins in figure 3 do not result in good rocking curves. As a result, it was only possible to measure the twin angle whilst heating the sample from room temperature, and not whilst cooling the sample from above T_C.

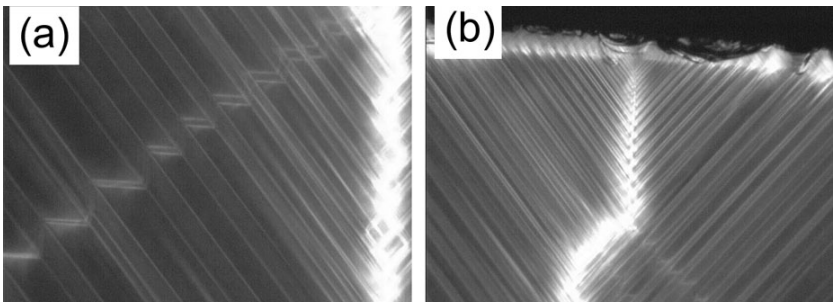

Figure 2. Typical optical micrographs of a (001) slice of $LaAlO_3$ as received from the manufacturer. The (110) edge of the crystal runs across the top of the right-hand image (b). The left-hand image (a) shows the dominant (100) twins, with a few (110) twins. The right-hand image (b) shows a boundary between regions with (100) and (010) twins. The field of view of the images is approximately 0.45 mm wide.

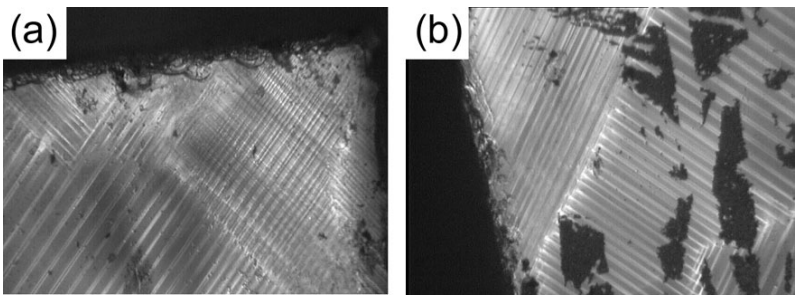

Figure 3. Typical optical micrographs of a (001) slice of $LaAlO_3$ after heating above $T_C = 550\,^{\circ}\mathrm{C}$. The maximum temperature reached is unknown. The (110) edge of the crystal runs across the top of the left-hand image (a), and the $(1\overline{1}0)$ edge can be seen to the left of the right-hand image (b). Both images show the mixture of (100) and (010) twins which make such crystals unsuitable for rocking experiments. The dark patches in (b) are remains of the metallic paste used to attach the sample to the diffractometer. The field of view of the images is approximately 0.45 mm wide.

In order to make samples like those shown in figure 3 more usable, an attempt was made to recover the lamellar microstructure. The sample was wrapped in Pt foil and then placed in a small mechanical clamp. The clamp applied a stress in the pseudocubic [100] direction. The clamped sample was then placed in an oven, and heated fairly rapidly ($\approx$20 K min^{-1}) to 850 K. This temperature was maintained briefly, and the oven was then left to cool back to room temperature. Once the sample was cooled, the clamp was removed, and the microstructure was rechecked with an optical microscope. As shown in figure 4, the stress favours one twin orientation, so that a simple lamellar microstructure results.

3.2. X-ray rocking experiments

Twinned samples of $LaAlO_3$, of the type shown in figure 2, were mounted on two-circle diffractometers, which are specially optimized for the collection of rocking curves. In these systems, the sample holder tilts around an axis perpendicular to the incident x-ray beam (the ω-axis of a standard four-circle diffractometer). The detector is an INEL 1D position-sensitive detector. The rocking experiment consists of measuring the diffracted intensity for a given Bragg reflection as a function of ω. Further details of the diffraction geometry are given in Locherer *et al* (1996), where the two-circle system is described as 'type X-1'.

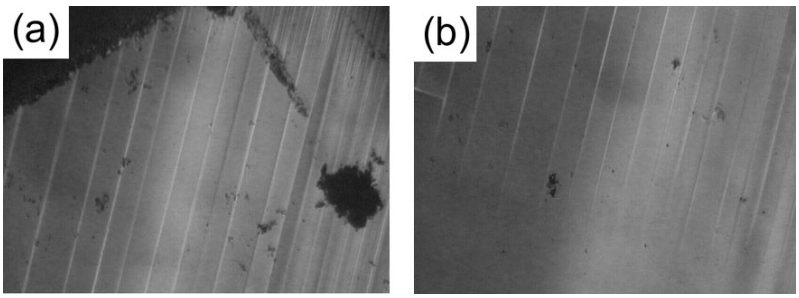

Figure 4. Typical optical micrographs of a (001) slice of $LaAlO_3$ after clamped heating to 580 °C. The (110) edge of the crystal runs across the top left corner of the left-hand image (a). Both images show predominantly (100) twins. The field of view of the images is approximately 0.45 mm wide.

Separate diffractometers were used to perform measurements at temperatures above and below room temperature. The low-temperature experiments were performed by placing the sample on a small nickel block (used to obtain the correct sample height), which was in turn mounted on a large copper block which was connected to a cryostat. The thermostat for the system was mounted within the copper block. Thermal contact between the sample, nickel and copper blocks was enhanced by the use of conducting paste. The whole assembly was put inside an evacuated chamber which gives a temperature stability of significantly better than ± 0.1 K. Measurements were made as the sample was cooled from room temperature, at 5 K intervals to $T = 10$ K.

For the high-temperature measurements, the sample was mounted on a Pt–Rd heating strip with a metallic paste. A small thermocouple situated on the underside of this strip immediately below the sample allows the temperature to be stabilized to ± 1 K. However, the system was only stable for $T > 420$ K, so no measurements were made between room temperature and 420 K. Above this temperature, measurements were made every 5–10 K up to the transition temperature, 850 K. However, the smallness of the peak splitting close to the transition temperature made it impossible to clearly resolve two peaks at temperatures above 750 K.

In each case, an as-received (001) slice of $LaAlO_3$ with (010) lamellar twins was mounted on the diffractometer, with the ω rocking axis parallel to [100]. In this configuration, the (010) twins are perpendicular to the incident x-ray beam. The intensity of the strong basal reflection 001 was then measured as a function of ω, with a step size in ω of 0.001°. For this combination of conditions, two peaks are expected in the intensity versus ω graph, each corresponding to one of the two domain orientations being in the diffraction condition. The only contribution to the splitting comes from the slightly different orientation of the (001) plane in the two domains.

4. Results

4.1. Changes in the rocking curve as a function of temperature

Figure 5 shows a representative selection of the rocking curves for $LaAlO_3$ at various temperatures. In all these measurements, the diffraction maxima from the two domains are clearly resolved, so the spontaneous strain may be determined from the peak splitting with little difficulty.

Two features of figure 5 are experimental artefacts. The reduction in the diffraction peak intensity with temperature is due to the fact that the control of the diffraction geometry

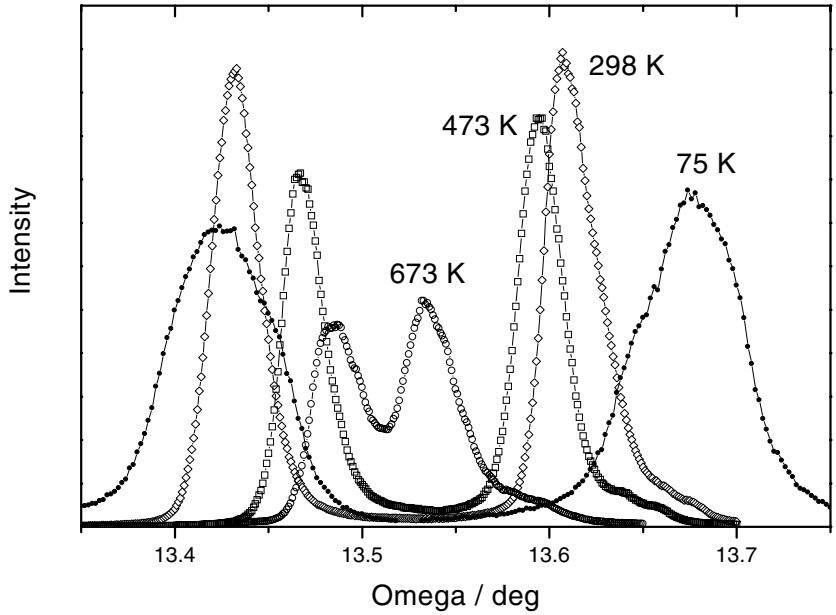

Figure 5. Typical rocking curves in $LaAlO_3$ at various temperatures.

is slightly compromised to permit enhanced temperature control. In the high-temperature experiments, the sample is attached directly to the resistance heater, which expands slightly at high temperature. Good temperature control is maintained, but the sample moves slightly away from the centre of the incident x-ray beam, leading to a reduction in diffracted intensity. Of course, this does not affect the measured peak spacing.

The low-temperature rocking curves had uniformly broader peaks than those measured on the high-temperature diffractometer. This is due to machine effects rather than changes in the sample. One factor is that the beam characteristics on the two diffractometers used are somewhat different. Another consideration is that the amorphous polymer used for the x-ray window material in the low-temperature sample chamber tends to crystallize over time, which broadens the diffraction peaks.

4.2. Peak splitting as a function temperature

The twin angle at each temperature was found by fitting the spectra shown in figure 5 to a pair of Gaussian functions. This process became difficult for T above about 700 K, and it proved impossible to determine meaningful separations above 750 K.

In order to compare these data with the studies of Chakoumakos *et al* (1998), Lehnert *et al* (2000) and Howard *et al* (2000), the lattice parameter data from these studies were converted from the trigonal setting to a pseudocubic setting. These results are shown in figures 6(a) and (b).

In figure 7, we compare the spontaneous strain measured by the rocking curve method with the results of neutron powder diffraction. The scaling between the two experiments is fixed by consideration of the unit cell geometry (equation (13) above), and not determined empirically. There is generally good agreement between the two types of measurement, except in the immediate vicinity of T_C where the spontaneous strain is very small. It may be that

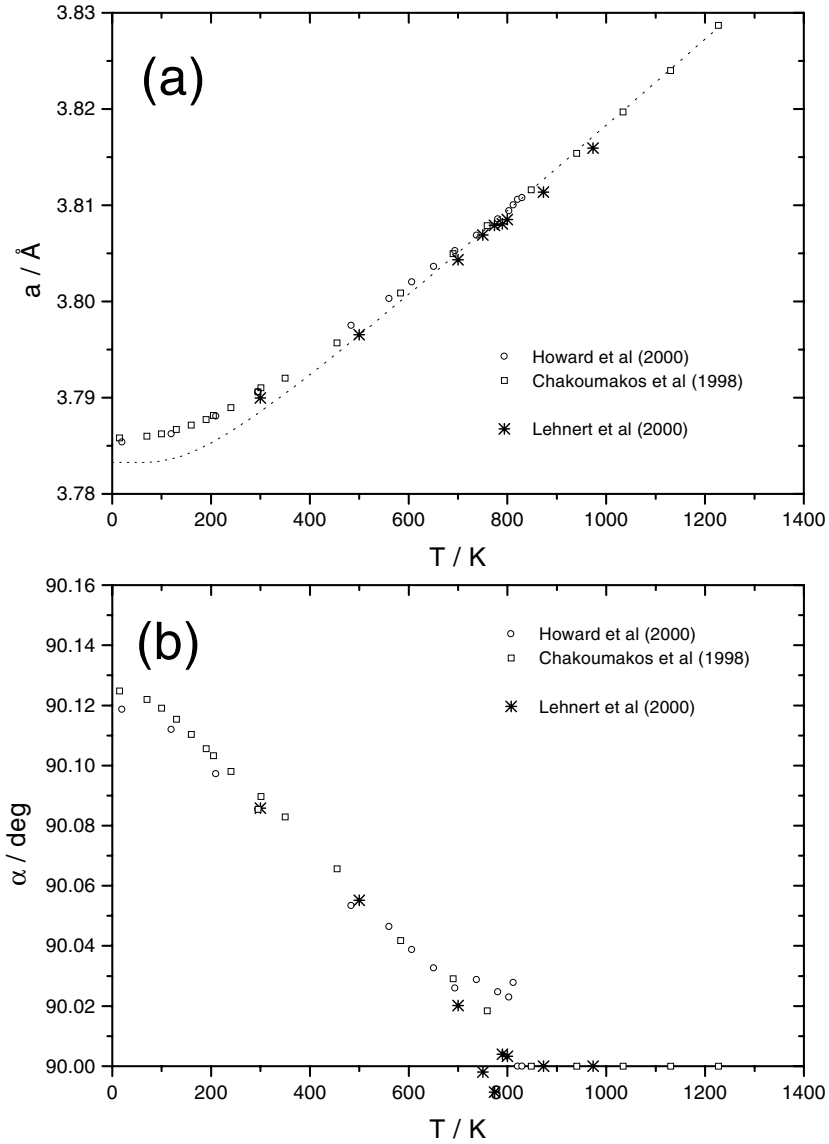

Figure 6. Temperature dependence of lattice parameters in $LaAlO_3$, from Howard *et al* (2000) (which includes data measured by Chakoumakos *et al* (1998)) and Lehnert *et al* (2000), using the cubic/pseudocubic setting throughout. In (a) the broken curve shows the bare thermal expansion, $a_0(T)$, fitted to the Chakoumakos *et al* (1998) and Howard *et al* (2000) data for $T > T_C$, and then forced to saturate with $\theta_S = 250$ K.

the lattice parameter data are compromised by overlap effects in the Rietveld analysis of the powder diffraction data. The extreme difficulty of measuring small deviations from the aristotype structure must be borne in mind when using these results to study the possibility of non-classical critical effects. A further point to note is that certain of the data of Lehnert *et al* (2000) appear to have been misrefined, since the points at 750 and 775 K have a positive value of e_4, whereas all the other data have e_4 negative.

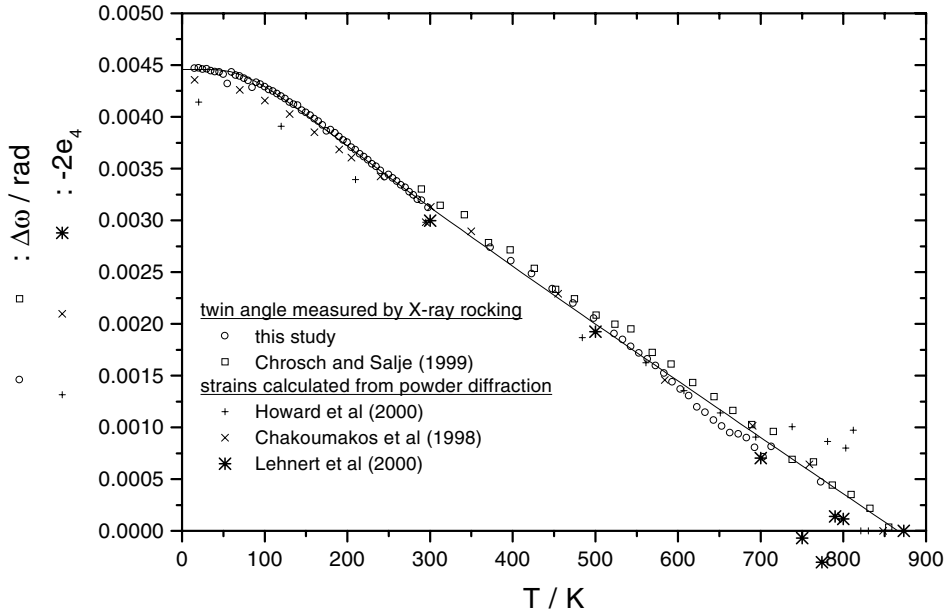

Figure 7. Temperature dependence of the spontaneous strain (e_4) measured by x-ray rocking diffraction (this study, and Chrosch and Salje (1999)), and neutron powder diffraction (Chakoumakos *et al* 1998, Howard *et al* 2000, Lehnert *et al* 2000). To facilitate the comparison, the twin angle $\Delta\omega$ and $-2e_4$ are plotted; these two quantities are expected to be equal. The fit (solid curve) is to a model of two processes with different saturation temperatures. The model parameters have been determined by reference to other experimental data only, and have not been optimized for the x-ray rocking data.

5. Discussion

The $Pm3m$–$R\bar{3}c$ phase transition in $LaAlO_3$ is well described by a second-order Landau potential at high temperatures, and shows the expected saturation of the order parameter at low temperatures. Fitting the twin angle data over the entire temperature range to the model in equation (4) above leads to the best-fit parameters $T_C = 834(2)$ K, $\theta_S = 95(4)$ K. Previously published values of T_C have typically been in the range 800–850 K.

The situation for the saturation parameter is more complex. If we consider the EPR (Müller *et al* 1968) and neutron diffraction (Howard *et al* 2000) data for $LaAlO_3$, we can determine values of θ_S for each symmetry-breaking process independently (figures 8 and 9). Although there are discrepancies between the two data sets, two points are clear. First, the saturation temperatures of the two processes are different: 260–400 K for rotation, and 150 K for distortion. The second point is that both these values are higher than the observed saturation of the spontaneous strain.

Similar results are obtained from measurements of the Raman spectrum of $LaAlO_3$ as a function of temperature (Salje *et al*, personal communication). $LaAlO_3$ has two soft Raman modes (Abrashev *et al* 1999); the E_g mode ($\omega = 34$ cm^{-1} at room temperature) and the A_{1g} mode (132 cm^{-1} at room temperature). Following the frequencies of these modes as a function of temperature, we find that θ_S for the E_g mode is 242 K, whilst θ_S for the A_{1g} mode is 156 K.

One way of resolving the discrepancy between the saturation temperatures is to describe the transition with two distinct processes, represented by two order parameters; for example, the

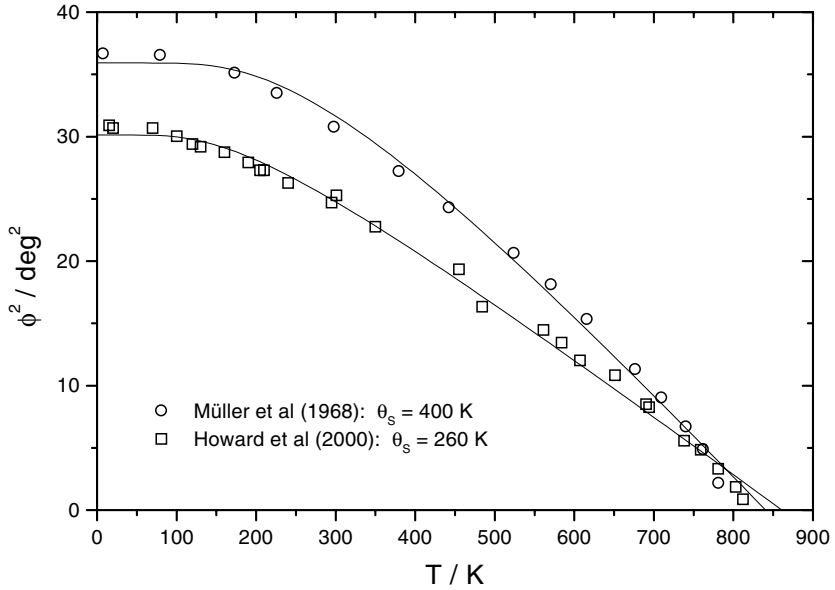

Figure 8. Temperature dependence of the AlO_6 rotation angle in $LaAlO_3$ measured by EPR spectroscopy (Müller *et al* 1968) and neutron diffraction (Howard *et al* (2000), including analysis of data from Chakoumakos *et al* (1998)). The fits are to a second-order Landau potential, modified by quantum saturation effects.

rotation and distortion of the octahedra. The measured spontaneous strain is then a function of the strains associated with each order parameter. In the lowest order, bilinear coupling is allowed by symmetry. In addition, biquadratic coupling (for example, via the symmetry breaking strain) is expected to occur.

In the simplest case of weak biquadratic coupling (Salje and Devarajan 1986), the total spontaneous strain from the phase transition is simply the sum of the spontaneous strains from the two component processes, and these follow simple second order potentials. Using equation (13) above, we can express the temperature dependence of the twin angle as

$$\Delta\omega = k_D\left(\coth\left(\frac{\theta_{SD}}{T_C}\right) - \coth\left(\frac{\theta_{SD}}{T}\right)\right) + k_R\left(\coth\left(\frac{\theta_{SR}}{T_C}\right) - \coth\left(\frac{\theta_{SR}}{T}\right)\right), \tag{14}$$

where k_D and k_R are prefactors associated with the twin angles which would result from bare rotation and distortion respectively, θ_{SD} and θ_{SR} are the saturation temperatures of the two processes, and T_C is the common transition temperature. For the Howard *et al* (2000) data in figures 8 and 9, $T_C = 866$ K. From figures 8 and 9, and Raman spectroscopy data (Salje, personal communication), the saturation parameters are $\theta_{SD} = 150$ K and $\theta_{SR} = 260$ K. The parameters k_D and k_R are fixed by the magnitudes of the rotation angle and distortion factor, and their contribution to the spontaneous strain (cf equation (13)). In figure 7, we compare the model of $\Delta\omega(T)$ based on two non-interacting processes with different θ_S values with the results of the high-resolution x-ray diffraction experiment. All the parameters in equation (14) have been determined by fitting the neutron diffraction data (Howard *et al* 2000), and so no attempt has been made to optimize the fit of the model to the x-ray diffraction data.

The contributions of the two processes to the overall spontaneous strain, and the origin of the anomalously low value of θ_S resulting from the strain measurements, are summarized in figure 10. At high temperatures (region (i) in figure 10) the contributions of both the rotation

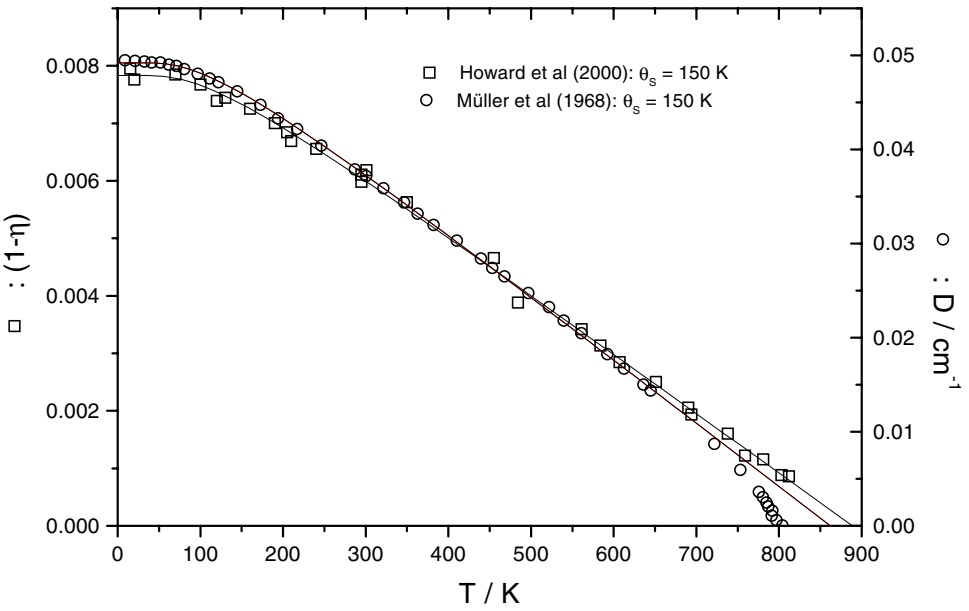

Figure 9. Temperature dependence of the AlO_6 distortion factor in $LaAlO_3$ measured by EPR spectroscopy (Müller *et al* 1968) and neutron diffraction (Howard *et al* (2000), including analysis of data from Chakoumakos *et al* (1998)). The fits are to a second-order Landau potential, modified by quantum saturation effects.

and distortion to the spontaneous strain are proportional to $|T_C - T|$, and so the total strain is also linear with temperature. At intermediate temperatures (region (ii)), the rotation has begun to saturate, but the distortion is still behaving classically. The effect is that the total spontaneous strain has a higher gradient in region (ii) than region (i). Finally, at very low temperatures, both component order parameters are independent of temperature, and the total strain saturates (region (iii)).

As shown by equations (3) and (4) above, one way of defining θ_S is in terms of the depression of Q at 0 K relative to the results of a simple classical extrapolation. On this measure, fitting behaviour of the type shown in Figure 10 to a single order parameter will give a very low apparent value of θ_S. The reason for this is the rapid increase in the spontaneous strain which occurs in the temperature range where one process is saturated and the other is active (region (ii) in figure 10).

Preliminary attempts to determine these parameters can be made on the basis of the existing data. Fitting the specific heat data of Schnelle *et al* (2001) to an Einstein model produces a rather poor fit, but the best fit Einstein temperature is $\theta_E = 515$ K. Taking an average phonon frequency from the lattice dynamics calculations of Abrashev *et al* (1999), and correcting for the low-frequency acoustic modes, we obtain $\theta_E = 530$ K. As noted in figure 6(a) above, the bare thermal expansion of $LaAlO_3$ (i.e. what would happen without the effect of the phase transition) has a plausible form if fitted to a model with $\theta_S = 250$ K, which would correspond to $\theta_E = 500$ K.

For the quantities associated with the order parameter, we determine θ_S, noting that in the simplest case of a simple acoustic soft mode coupled to all the hard modes we expect $\theta_S = \theta_{E/2}$ (Salje *et al* 1991, Dove *et al* 1992). The best estimates we have for the saturation of the rotation and distortion are 260 and 150 K respectively. Combining these two parameters

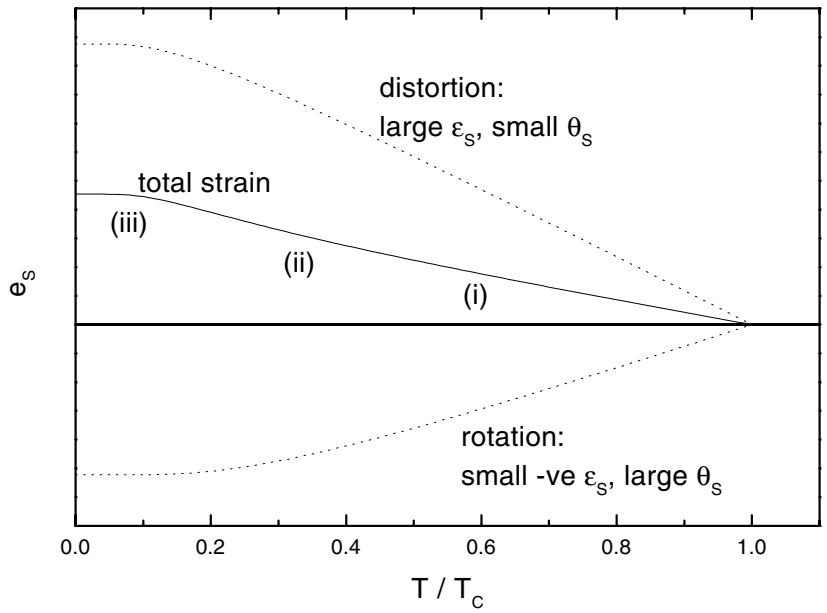

Figure 10. Schematic form of the spontaneous strain components, and resulting total spontaneous strain in $LaAlO_3$. In region (i), both component processes are behaving classically. At lower temperatures (region (ii)), the rotation has begun to undergo quantum mechanical saturation, but the distortion is still behaving classically. At very low temperatures (region (iii)), both processes are saturated.

to describe the overall symmetry-breaking strain shows that while these parameters are not unreasonable, the fit of the model to high-resolution data could be improved by adjusting the parameters slightly.

In this study, we have measured the symmetry-breaking spontaneous strain in $LaAlO_3$ by a high-precision, high-accuracy technique. These data agree with the results of earlier studies at high temperatures, but the low-temperature data cannot be described consistently by a Landau-like model with a single order parameter. However, two order parameters, with different quantum mechanical saturation properties, appear to be sufficient to explain all the observations. The values of the saturation temperatures for the various physical properties of $LaAlO_3$ provide insights into the microscopic mechanisms driving the behaviour of this material. However, to determine these in a rigorous manner requires high-precision data for the variation of the AlO_6 distortion factor and rotation angle as a function of temperature. Further investigations are planned.

References

Abrashev M V, Litvinchuk A P, Iliev M N, Meng R L, Popov V N, Ivanov V G, Chakalov R A and Thomsen C 1999 Comparative study of optical phonons in the rhombohedrally distorted perovskites $LaAlO_3$ and $LaMnO_3$ *Phys. Rev.* B **59** 4146–53

Beuble S, Knorr K, Brecht E and Schmahl W W 1998 Influence of the ferroelastic twin domain structure on the {100} surface morphology of $LaAlO_3$ HTSC substrates *Surf. Sci.* **400** 345–55

Born M and Huang K 1954 *Dynamical Theory of Crystal Lattices* (Oxford: Clarendon)

Carpenter M A, Salje E K H and Graeme-Barber A 1998 Spontaneous strain as a determinant of thermodynamic properties for phase transitions in minerals *Eur. J. Mineral.* **10** 621–91

Chakoumakos B C, Schlom D G, Urbanik M and Luiane J 1998 Thermal expansion of $LaAlO_3$ and (La, Sr)(Al, Ta)O_3, substrate materials for superconducting thin-film device applications *J. Appl. Phys.* **83** 1979–82

Chrosch J and Salje E K H 1999 Temperature dependence of the domain wall width in $LaAlO_3$ *J. Appl. Phys.* **85** 722–7

Dove M T, Gambhir M and Heine V 1999 Anatomy of a structural phase transition: theoretical analysis of the displacive phase transition in quartz and other silicates *Phys. Chem. Min.* **26** 344–53

Dove M T, Giddy A P and Heine V 1992 On the application of mean-field and Landau theory to displacive phase transitions *Ferroelectrics* **136** 33–49

Geller S and Bala V B 1956 Crystallographic studies of perovskite-like compounds. II. Rare earth aluminates *Acta Crystallogr.* **9** 1019–25

Hayward S A and Salje E K H 1998 Low-temperature phase diagrams: non-linearities due to quantum mechanical saturation of order parameters *J. Phys.: Condens. Matter* **10** 1421–30

Howard C J and Kennedy B J 1999 The orthorhombic and rhombohedral phases of $LaGaO_3$—a neutron powder diffraction study *J. Phys.: Condens. Matter* **11** 3229–36

Howard C J, Kennedy B J and Chakoumakos B C 2000 Neutron powder diffraction study of rhombohedral rare-earth aluminates and the rhombohedral to cubic phase transition *J. Phys.: Condens. Matter* **12** 349–65

Lehnert H, Boysen H, Schneider J, Frey F, Hohlwein D, Radelli P and Ehrenberg H 2000 A powder diffraction study of the phase transition in $LaAlO_3$ *Z. Kristallogr.* **215** 536–41

Locherer K R, Hayward S A, Hirst P J, Chrosch J, Yeadon M, Abell J S and Salje E K H 1996 X-ray analysis of mesoscopic twin structures *Phil. Trans. R. Soc.* A **354** 1–31

Megaw H D and Darlington C N W 1975 Geometrical and structural relations in the rhombohedral perovskites *Acta Crystallogr.* A **31** 161–73

Müller K A, Berlinger W and Waldner F 1968 Characteristic structural phase transition in perovskite-type compounds *Phys. Rev. Lett.* **21** 814–17

Pérez-Mato J M and Salje E K H 2001 Order parameter saturation at low temperatures: displacive phase transitions with coupled Einstein oscillators *Phil. Mag. Lett.* **81** 885–91

Romero F J *et al* Quantum saturation of tetrahedral rotations in quartz, in preparation

Salje E K H 2000 Quantum saturation of the spontaneous polarisation in ferroelectric materials *Fundamental Physics of Ferroelectrics* ed R E Cohen (New York: American Institute of Physics) pp 297–303

Salje E and Devarajan V 1986 Phase transitions in systems with strain-induced coupling between two order parameters *Phase Transitions* **6** 235–48

Salje E K H, Wruck B and Thomas H 1991 Order-parameter saturation and low-temperature extension of Landau theory *Z. Phys.* B **82** 399–404

Schnelle W, Fischer R and Gmelin E 2001 Specific heat capacity and thermal conductivity of $NdGaO_3$ and $LaAlO_3$ single crystals at low temperatures *J. Phys. D: Appl. Phys.* **34** 846–51